YTUP

Journal of Thermal Engineering
https://jten.yildiz.edu.tr/
https://doi.org/10.47481/jten.0021

RESEARCH ARTICLE

Simulation of air flow behavior and its influence on thermal comfort for a naturally ventilated passenger railway coach in India

Shashank Shekhar Mishra[1] Vivek Kumar Gaba[2] Nisha Netam[3,*]

[1]Department of Mechanical Engineering, National Institute of Technology, Raipur, Chhattisgarh, 492010, India
[2]Department of Mechanical Engineering, National Institute of Technology, Raipur, Chhattisgarh, 492010, India
[3]Department of Mechanical Engineering, National Institute of Technology, Raipur, Chhattisgarh, 492010, India

Abstract

This study investigates thermal comfort parameters at different locations within a moving, non-air-conditioned railway coach in India. The internal environment of a ventilated railway coach is highly dynamic, making it difficult to predict accurately the relative thermal comfort conditions at different locations within the coach. This study combines computational fluid dynamics (CFD) with field measurements to evaluate real-time environmental parameters and their effects on thermal comfort for different seat orientations on a moving train. Given the dynamic environment of ventilated moving stock, the results provide crucial inputs for the design optimization of non-air-conditioned railway coaches. The results reveal a turbulent airflow, predominantly influenced by the window air inlet, resulting in small but significant temperature variations across seat locations in the compartment. Upper seats were the hottest, whereas the central area beneath the overhead vents was cooler. Validation of simulation results against experimental data indicates a satisfactory correlation, with mean errors within 10%. Notably, temperature measurements indicate the presence of heat plumes, particularly around the walls, while the central area beneath the overhead vent is the coolest, exhibiting only a slight temperature difference of 1.37^{O}C across the compartment. Mean air velocity was 0.364 m/s; exceeding the ASHRAE standard. It was influenced by the compartment's design and airflow turbulence, with maximum velocities near windows and stagnant zones in the aisle. The analysis highlights the importance of localized thermal sensations, radiant asymmetry, and vertical temperature differences in shaping passengers' perception of comfort. The mean standard effective temperature for the coach is found to be 36.65^{O}C while the mean predictive mean vote of passengers is found to be 4.73. The true novelty of the work lies in identifying specific discomfort zones within ventilated railway coaches and thereby providing a clear insight into improving the thermal comfort of passengers travelling in non-air-conditioned railway coaches. The study concludes that improving airflow management and addressing psychological aspects of thermal comfort can significantly enhance overall comfort in railway coaches and offer valuable insights for future design and operational enhancements in railway passenger transport.

Keywords: Thermal comfort, cfd simulation, non-air-conditioned railway coach, pmv, ppd

Cite this article as: Mishra, S. S., Gaba, V. K., & Netam, N. (2026). Simulation of air flow behavior and its influence on thermal comfort for a naturally ventilated passenger railway coach in India. Journal of Thermal Engineering, 12(3), 1159–1171. https://doi.org/10.47481/jten.0021

1. Introduction

According to Centre of Railway Information System(CRIS), around 40 Lakh seats of Indian railway are in non-air conditioned coaches[1]. The figure accounts for approximately 70% of the total seating capacity of Indian passenger trains. In all these coaches, passengers' thermal comfort is primarily influenced by window-air ventilation. Unfortunately, no significant design optimizations have been made for ventilated railway coaches with respect to thermal comfort. Despite the phenomenal growth and expansion, the ventilated coaches of Indian Railways seem essentially the same as when they were first introduced 170 years ago. To improve the thermal comfort of passengers, it is essential to have direct, accurate, and available data on the existing railway coach and its environmental conditions. ASHRAE advocates for subjective evaluation of thermal comfort, stating thermal comfort as a personal articulation of satisfaction with the thermal environment [2].

*Corresponding Author
E-mail Adress: nishane.me@nitrr.ac.in

Submitted: 02 October 2025; **Accepted:** 09 November 2025

This paper was recommended for publication in revised form by Editorin-Chief Ahmet Selim Dalkılıç

However, the human sense of thermal comfort is diverse and complex and thus must be validated by experimental and computational results.

Several studies have evaluated occupants' thermal comfort. However, an extensive review of the literature reveals that thermal comfort studies are more inclined toward static enclosed environments, such as buildings or office spaces, than toward dynamic open spaces such as ventilated rolling stock. Regarding passengers' thermal comfort, very few key studies have been conducted in India and abroad.

The early evidence of thermal comfort study of trains is found in the work of XJ Ye[29]in 2004. However, the coaches selected for the study were air-conditioned coaches from high-speed trains in China; where the coach environment is a controlled environment with temperature ranging from 23^{O}C to 28^{O}C, which is within the general acceptable comfort temperature band. Thus, almost 71% of passengers found the exposed environment and the air quality acceptable. Yet another field study of Chinese railway was carried out by Chunqing Wang[30]during summer of 2018 and 2019 where 717 survey samples were collected from Changchun, metro stations, China. Understanding temperature, analyzing passenger responses, identifying comfort zones, and providing a data foundation for metro system design and administration in cold climates were among the objectives. Yuchun Zhang[31] in 2020, carried out experiments to study transient thermal comfort when stepping outdoors.

Researchers shifted from conventional field studies to software simulations of thermal environments following the introduction of computational fluid dynamics (CFD). Since then, CFD has been one of the most significant tools for analyzing and validating thermal and built environments and has been widely used by numerous scholars. Z Geet. al[3]simulated a natural ventilation condition for school building in Singapore using ANSYS Fluent (v17.2). In a similar study Netam et. al.[4] performed similar simulation study using passive cooling techniques for static building environment located at same climatic zone and validated the results with the experimental results. A review of the available literature in the field suggests that thermal comfort models originally developed for buildings have also been applied to vehicles.

Predictions of thermal comfort in cars [5],[6]ventilation, air conditioning (HVAC, [7], [8]have been carried out by several scholars including Huizenga et al.[9] who combined the CFD program FLUENT with the Virtual Thermal Comfort Engineering(VTCE)tools. In[10]whereby fluctuations as well as anisotropy of the turbulence are represented with insufficient precision. This paper applies a thermal large eddy lattice Boltzmann method (LES–LBMwhereby fluctuations as well as anisotropy of the turbulence are represented with insufficient precision. This paper applies a thermal large eddy lattice Boltzmann method (LES–LBM, Reynolds-Averaged Navier-Stokes (RANS) simulations using the k-ε turbulence model and surface-to-surface radiation modeling were conducted for a car with two occupants. In this study, human thermal comfort was predicted using sensation indices. In [11]the thermal radiation and the thermal comfort in a complete double decker train cabin with 96 passengers are presented in this paper. The computations have been performed by coupling flow simulations conducted with the computational fluid dynamics (CFD, the thermal comfort in a full-size Sport Utility Vehicle (SUV) occupied with 6 passengers has been evaluated analyzing equivalent temperatures. Further, in [10], the thermal comfort in trains has been predicted based on unsteady RANS simulations with the commercial code Star-CD. The latter, includes the so-called TIM (German acronym for "Thermo-physiological Occupant Model"), which is based on the model by Stolwijk[12]. The capabilities of commercial thermal comfort models under aircraft cabin conditions have been evaluated in [8].However vehicle environment is very different form buildings environment, as it is affected by many more factors than the buildings (i.e. solar radiation, high air velocity, high differences between Finterior surfaces)[13]driver's thermal comfort must to be ensured to reduce both thermal stress (thus reduces the risk of accidents

Among the relevant work in the field, a handful of studies have focused on thermal comfort analysis of railway passenger cabins. Weiwei Liu[14]the dynamic cooling loads of YZ25G train compartment were investigated under the average ambient conditions during the hottest month July, when it travels in three main railway lines of China. The effects of ambient conditions and body thermal storage on the variation in the cooling load were discussed. The results indicated that the maximum total cooling loads were between 40.4 and 43.8 kW, and the minimum between 4.5 and 33.7 kW. And significant differences in dynamic cooling load of train compartment were found between different regions (north/south and west/east, found that all the studies carried out for passenger trains considers a steady thermal environment inside the train cabin and thus China MOR standard (TB1951-87) has been followed. In contrast, the thermal environment inside long-distance moving trains is not steady, and thus the results of TB1951-87 cannot reflect the variation in the cooling load for a train during travel. In a recent attempt Alam et. al [32] focused his interest towards exploring thermal comfort for Indian railways, but his studies were limited to pantry kitchen of the railways. The kitchen environment is entirely different from the passenger-occupancy space. The obvious interpretation of the above studies suggests that to date no significant contributions have been made towards occupants in ventilated, moving railway coaches, particularly under the composite climatic conditions observed in central India.

This study attempts to fill the research gap concerning passengers' thermal comfort inside a ventilated, moving railway coach. The present study aims to evaluate the real-time environmental parameters for different seat orientations inside a moving train and their effect on occupants' thermal comfort.

2. Materials and Methods

2.1. Overview of selected railway coach for the investigation

The railway coach selected for the purposes of the investigation is an Integral Coach Factory coach (popularly known as ICF coach) that has a metallic shell-type structure. The passenger compartment of the coach is 3.25 meters wide, 2.73 meters high and 16.28 meters long (excluding the lavatory section). For air ventilation, windows measuring 610 mm wide and 560 mm high, with operable shutters, are mounted on the two side walls at an elevation of 710 mm above the floor. A conventional coach comprises a total of 18 such windows on either side of the passenger compartment. Circular ducts are provided in the ceiling of the coach (typically 5) for ventilation purposes. The detailed dimensions of the selected coach are shown in Figure 1. The second-class, non-air-conditioned ICF coach selected for the study has single-tier seats for seating purposes and is equipped with overhead luggage racks, as depicted in the figure.

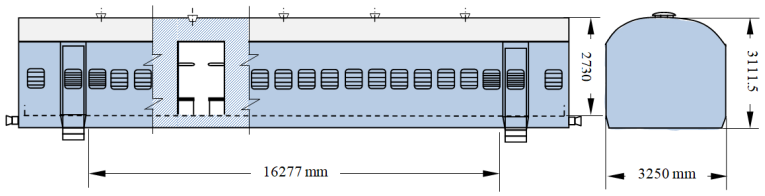

Figure 1. Dimensions of the selected coach

2.2. Recording environmental parameters

Field measurements were taken on April 23rd - 2023, at 09:30 Hrs. at Bhilai Nagar station where the axis orients track from south-west to north-east and the direction of wind was found to be towards west. Other meteorological measures include recording of dry bulb temperature (^{O}C), barometric pressure(bar), relative humidity (%), wind velocity(m/s) and solar radiation (W/m^2). All readings were taken outside the coach at a height of 150 cm above the ground, while the train was halted at the platform. The same is depicted in Table 1 below. To validate the simulation results, indoor environmental parameters were recorded under moving-train conditions. These include measurements of indoor air temperature, indoor surface temperature, globe temperature, air velocity, and relative humidity at different spatiotemporal points. Same has been depicted in Table 1b on the subsequent page.

Figure 1. a. Measurement instruments used to obtain environmental parameters

Table 1. a. Outdoor environmental parameters

Location	Longitude	Latitude	Time	Date	Solar Irradiation	DBT	Wind Velocity	Humidity	Wind Direction	Barometric pressure
Bhilai	81.35° E	21.19° N	09:15 Hrs	April 13,2023	544.7 W/m^2	34 ^{O}C	5.6 km/hr	55 %	278^{O}	1.008 bar

Figure 2 depicts measurement points within the coach. Surface temperatures were measured using a duly calibrated digital infrared thermometer along with contact-type thermocouple temperature sensors, which were placed on the inner surface of the coach, preferably near windows, ceilings, and different parts of the seats (three-digit number with prefix 'S'). Similarly, a Testo 410-2 hand-held temperature sensor was used to record air temperature at different probe points shown in the following figure.

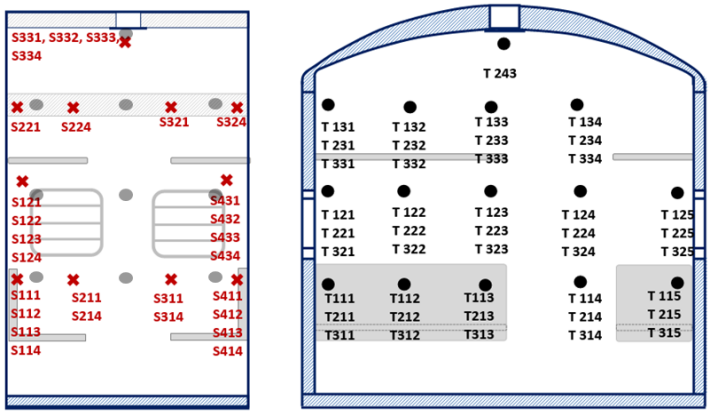

Figure 2. Measurement points inside the coach

Forty-three (43) probe points were identified based on passenger locations within the coach. All such probe points are designated by a three-digit number prefixed with 'T' in the diagram. The digits of the number denote the coordinates on X, Y, and Z axes, respectively. For example, a probe point designated by T213 represents second (2^{nd}) point in X axis, 1^{st} point in Y axis and 3^{rd} point in Z axis. A single-compartment unit is designed to accommodate 8 seated passengers, including four in window seats. Apart from this, luggage racks above the seats are also used for seating during periods of congestion. Considering, a total of 14 probe points were marked, each a few centimeters below the passengers' face level. Other probe points were placed at suitable distances and heights in the gallery between the passengers' seats, which is an unobstructed space allowing ventilated airflow. The Testo 410-2 sensor also measures wind velocity and relative humidity. Air velocity is measured perpendicular to the wind direction. All the fans were initially kept switched off during data collection to avoid interference with natural ventilation.

Table 1. b. Measurement of indoor thermal comfort parameters

Parameters	Description of the Device	Operative range	Accuracy	Measurement Points
Air Temperature (t_a)	Testo 410-2 hand held Temp. Sensor	-10°C - 50°C	±0.5°C	T111-T243
Relative Humidity (RH)	Testo 410-2 hand held Humidity Sensor	0 to 100 %	±2.5 % rh, 0.1% resolution	T111-T243
Air velocity(v_a)	Testo 410-2 hand held Anemometer	0.4 to 20 m/s	±0.2 m/s + 2 % of m.v.	T111-T243
Globe Temperature(t_g)	In house made GT with 10 cm dia. Copper black ball and calibrated digital thermometer	-50°C - 300°C	±0.5°C	T221, T222, T223, T224,T225
Surface temperature(t_s)	1. GM333A Portable Digital Infrared Thermometer	-50°C - 400°C	±1.5°C	S111 – S334
	2.Sigma digital thermocouple temperature sensor	-50°C - 110°C	±1.5°C	S111 – S334
Solar radiation	LX 107 Solar Power Meter	2000 W/m²	0.1 W/m²	-

2.3. Modeling of railway coach for simulation

The academic version of DSS Solid Works has been used to model a railway coach. ICF coach manuals and codes published by Rolling Stock Knowledge Resource[15] have been referred to for the dimensions and drawing of the coach. The passenger section of a typical ICF coach is subdivided into 9 identical compartments. To conserve computational resources, only a single compartment has been modeled and has been further simplified by eliminating irrelevant components of the coach, such as holding bars, hooks, and bulbs. The same is shown in Figure 3.

The windows have been provided to accommodate velocity inlets in the coach, while the upper ceiling air vent has been defined as a pressure-opening outlet from the coach. The built-in discrete solar radiation module has been incorporated to account for the effect of solar radiation on the coach. The wall materials were selected as steel, while the internal flow geometry was described as a fluid(air) in the simulation. To accommodate the effect of heat flux from the human body, internal heat source of 58 W/m^2 was defined in the model.

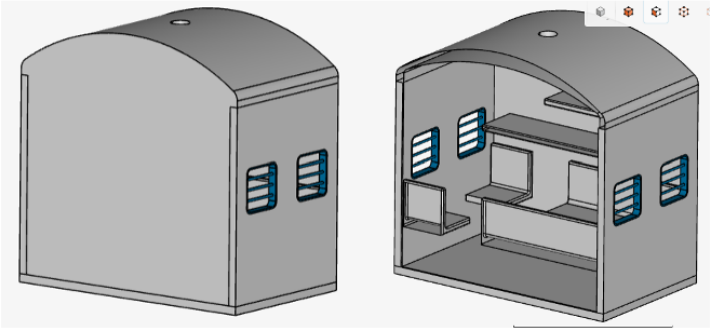

Figure 3. Simplified Cad Model of the coach compartment for simulation

2.4. Governing Mathematical Equations

The Navier-Stokes equations, together with the Boussinesq approximation, have been solved for the thermal flow field within the coach cabin. The equations were derived from the basic governing equations for mass, momentum, and energy as follows:

$$\frac{\partial \rho}{\partial t} + \nabla \cdot (\rho \vec{u}) = S_m \quad (1)$$

$$\frac{\partial}{\partial t}(\rho \vec{u}) + \nabla \cdot (\rho \vec{u}\vec{u}) = -\nabla_p + \nabla \cdot (\bar{\bar{\tau}}) + \rho \vec{g} + \vec{F} \quad (2)$$

$$\frac{\partial}{\partial t}(\rho E) + \nabla \cdot \{\vec{u}(\rho E + p)\} = \nabla \cdot \left(k_{eff} \nabla T - \left(\sum_j h_j \vec{J}_j + \bar{\bar{\tau}}_{eff} \cdot \vec{u}\right)\right) + S_h \quad (3)$$

In the above expression mass source is denoted by S_m, while the gravitational and external body forces are represented by $\rho\vec{g}+\vec{F}$ respectively. Effective conductivity is denoted by k_{eff} and $\bar{\bar{\tau}}$ represents the stress tensor and is expressed as:

$$\bar{\bar{\tau}} = \mu\left[\left(\nabla \vec{u} + \nabla \vec{u}^T\right) - \frac{2}{3}\nabla \cdot \vec{u} I\right] \quad (4)$$

Where μ stands for dynamic viscosity while I represent unit tensor.

2.5. Boundary condition

Data gathered during field measurements served as the basis for the boundary conditions used in the simulation. Train number 07051 operates on weekends and has moderate occupancy between the selected stations. The first halt of the train comes after 50 minutes, giving ample time to take measurements under steady-state conditions. Once it departs from the selected station, it runs continuously for 37 km at an average speed of 44 km/hr. However, for simplicity, the train was considered stationary, and the train's speed was compensated by the airflow through the windows. The air velocity was thus measured at the center of the window levels by placing the anemometer parallel to the window frame. All four windows served as air inlets into the compartment, and the inlet air existed through vents in the ceiling. Thus, velocity-inlet and pressure-outlet boundary conditions have been defined for simulation purposes.

The internal air flow profile may be considered to follow the logarithmic law[3]as per the equations given bellow:

$$U(z) = \frac{u^*_{ABL}}{\kappa} \lessapprox \left(\frac{z + z_0}{z_0}\right) \quad (5)$$

Here u^*_{ABL} represents friction velocity and is accounted in terms of reference velocity U_{ref} measured at a height of h_{ref} and von Karman Constant as follows: ϰ (kappa)(0.42) as follows: ($z_0$being aerodynamic roughness)

$$u^*_{ABL} = \frac{\kappa U_{ref}}{\ln\left[\frac{h_{ref} + z_0}{z_0}\right]} \quad (6)$$

In a single compartment, window openings constitute approximately 9.4% of the total lateral surface area (excluding the floor). Around 13.16 m^2 of the outer surface area of the compartment, which is made up of IRSM-41/36 steel (up to 3.15 mm thick [16]is exposed to direct solar radiation and thus radiation model required to be included in the simulation. LX-107 hand-held solar power meter has been used to record the direct and diffuse solar irradiance at Bhilai Nagar station and the same has been found to be 226.4$W/m^2$and 318.3 W/m^2respectively. The train's windows face southeast and northwest, both diffuse and direct solar radiation were considered

in the simulation. Although windows are equipped with glass shutters, passengers mostly refrain from using them during the summer. Thus, during the study, all glass shutters were kept open, and the transmittance of the window glass was neglected. Also, for a relatively short period during the study, fluctuations in solar irradiance were negligible.

Table 2. Boundary conditions for the simulation

Boundary	Type	Heat transfer/ Temperature	Mass and momentum	Radiation
Window 1	Velocity Inlet	$T_o = 34^OC$	$V_x = 8.0$ m/s $V_y = 0$ m/s	-
Window 2	Velocity Inlet	$T_o = 34^OC$	$V_x = 8.0$ m/s $V_y = 0$ m/s	-
Window 3	Velocity Inlet	$T_o = 34^OC$	$V_x = 8.0$ m/s $V_y = 0$ m/s	-
Window 4	Velocity Inlet	$T_o = 34^OC$	$V_x = 8.0$ m/s $V_y = 0$ m/s	-
Internal surfaces (including ceiling)	wall	$T_{wall} = 35^OC$ $h_c = 58$ W/m^{2}K	No slip wall	solar radiation = 534.7 W/m^2
Ceiling vent	opening		P = 1.008 bar	

During the daytime lights are generally not being used inside the coach and fans were intentionally kept switched off during the study as mentioned earlier. Normally passenger prefer to remain seated in the lower seats and thus heat flux generated per passenger is considered to be 58 W/m^2[17]. Jelena Srebricet. al. [18]recommends the convective to radiative heat flux to be in ratio of 30:70, considering thus the values for the same has been taken into account are 17.4 W/m^2 and 40.6 W/m^2 respectively. Considering each passenger carrying smart phone with them, 2W heat generated per smart phone has not been taken into account because of the negligibly small value. All other components and objects inside the coach are adiabatic. The emissivity and diffuse fraction (a ratio between the diffuse reflected energy and the total reflected energy at an opaque boundary) of all surfaces inside the room were assumed to be 0.9 and 1.0 respectively. The temperatures at internal surfaces of the coach were considered as the mean measured value at all internal surface measurement points.

In addition, the solar load model was considered. The embedded model calculates the direction of the sun relative to the coach using the specified time, date, and location. The ambient conditions for a typical summer day chosen for analysis are presented in Table 2. The solar load model consists of a solar ray-tracing algorithm and a surface-to-surface (S2S) radiation model.

2.6. Setting up the simulation model

A single-phase, steady-state simulation model has been utilized to analyze the flow behavior of air within the coach compartment. The full buoyancy model, based on the ideal gas law for assessing fluid density, has been incorporated into the simulation.

Because of the turbulent nature of the flow inside the coach cabin, the Favre-averaged Navier-Stokes (FANS) equations have been incorporated into the solver, which involve the time-averaged effect of turbulence on flow parameters. In the process, an additional Reynolds stress term appears in the equation. The computational tool used for the simulation utilizes turbulent kinetic energy and its dissipation rate, using the k-ε model which is well known for showing great results in the free stream region[21].However, the selection of the k-ε model is predominantly affected by the complexity of the problem as well as by the capabilities and limitations of the available computational resources. Nevertheless, the simulation tool used incorporates a modified version of classical k-ε model proposed by Lam and Bremhorst [19] based on following conservation laws:

$$\frac{\partial \rho\varepsilon}{\partial t} + \frac{\partial \rho\varepsilon u_i}{\partial x_i} = \frac{\partial}{\partial x_i}\left(\left(\mu + \frac{\mu_t}{\sigma_\varepsilon}\right)\frac{\partial \varepsilon}{\partial x_i}\right) + C_{\varepsilon 1}\frac{\varepsilon}{k}\left(f_1 \tau_{ij}^R \frac{\partial u_i}{\partial x_j} + C_B \mu_t P_B\right) - f_2 C_{\varepsilon 2}\frac{\rho\varepsilon^2}{k} \quad (7)$$

$$\tau_{ij} = \mu s_{ij} \quad \tau_{ij}^R = \mu_t s_{ij} - \frac{2}{3}\rho k\delta_{ij}, \quad s_{ij} = \frac{\partial u_i}{\partial x_j} + \frac{\partial u_j}{\partial x_i} - \frac{2}{3}\delta_{ij}\frac{\partial u_k}{\partial x_k} \quad (8)$$

$$P_B = -\frac{g_i}{\sigma_B}\frac{1}{\rho}\frac{\partial \rho}{\partial x_i} \quad (9)$$

Here C_μ =0.09, $C_{\varepsilon 1}$ = 1.44, $C_{\varepsilon 2}$ =1.92, σ_k =1, σ_ε =1.3, σ_B =0.9, and C_B =1 if P_B<0, CB =0 if PB<0.The turbulent viscosity term in the above expression is determined from:

$$\mu_t = \rho C_\mu f_\mu \frac{k^2}{\varepsilon} \quad (10)$$

Where f_μ is the Lam and Bremhorst's damping function and is obtained from:

$$f_\mu = [1 - \exp(-0.0165R_y)]^2 \cdot \left(1 + \frac{20.5}{R_t}\right) \quad (11)$$

Where $R_t = \frac{\rho k^2}{\mu\varepsilon}$

3. Verification of the simulation model

3.1. Test for Mesh independence

The grid independence study of indoor air temperatures was performed to verify the CFD model solution. Three meshes, successively refined (maximum element sizes for the course, medium, and fine meshes were 0.21 m, 0.10 m, and 0.066 m, respectively), were created using mostly structured grids. The refinement ratio (r) for a 3D mesh is defined as the ratio between the number of grid elements in the fine (Δ_{fine}) and coarse (Δ_{coarse}) meshes.

$$r = \left(\frac{\Delta_{fine}}{\Delta_{coarse}}\right)^{1/3} \quad (12)$$

It is recommended that the grid refinement ratio must be greater than 1.3 [22]the Fluids Engineering Division of ASME has pursued activities concerning the detection, estimation and control of numerical uncertainty and/or error in computational fluid dynamics (CFDto allow the discretization error to be separated from the other sources of error. The number of grid elements (Δ) and the refinement ratio (r) for each mesh are presented in the table below.

Table 3. Number of grid elements (Δ) and the refinement ratio(r) for each mesh

coarse	medium	fine	r_{32}	r_{21}
479289	1066002	2480318	1.31	1.33

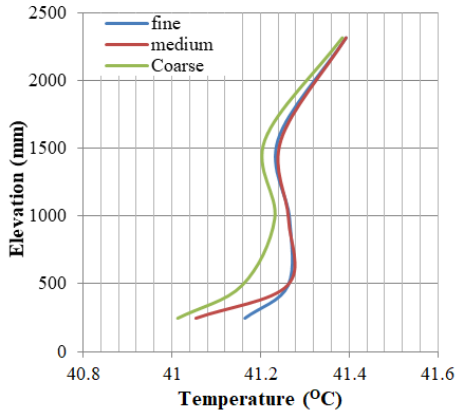

Figure 4. Temperature variation along elevation with different mesh settings

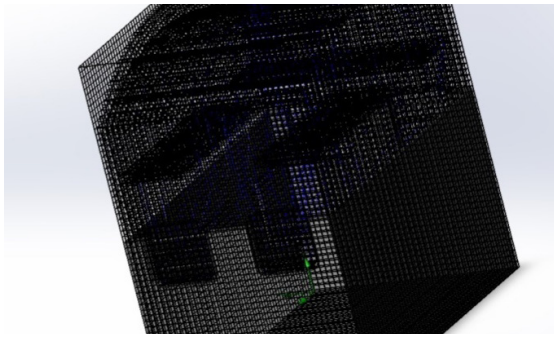

Figure 5. Grid model of coach compartment with medium grid size

To verify the mesh quality, the model was simulated to assess temperature variation along the elevation of the central part of the coach compartment using all three mesh settings. The variation in the results is shown in Figure 4. For the medium and fine meshes, temperature converges satisfactorily at higher elevations. Even at the lower elevation of the coach temperatures obtained with medium grids are very similar to those obtained with fine grids. The mean percentage error between results obtained with medium and fine grids is only 0.05%, which illustrates that the results are independent of grid size. Thus, the simulation is performed using medium-sized grids to optimize computational cost and time. Figure 5 depicts the grid model of the coach compartment with a medium grid size.

3.2. Validation of the simulation results

For validating the results, the simuated values of air velocity and temperature are compared with the experimentally obtained values of air velocity and temperatures of the same measurement points. For quantitative error analysis, deviation is expressed in terms of root mean square percent error (RMSPE) as follows:

$$e = \sqrt{\frac{\sum_{i=1}^{n} || y_{sim(i)} - y_{exp(i)} ||^2}{n}} \quad (13)$$

Where i = 1 to n (number of data)

Following figure number 6-a represents the comparision of root mean squared percentage deviation between measured and simulated values of air velocity and temperature.

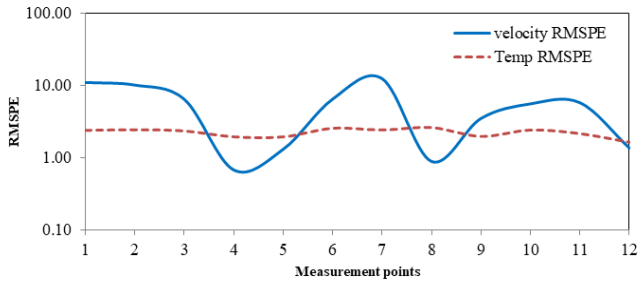

Figure 6. a. Root mean squared percentage error for simulated and measured velocity and temperature values

The e value for velocity is 5, and for temperature is 2.24. The e values mentioned above seem highly promising compared with similar previous studies. For instance Netam et. al [27] reports e value in the range of 2.2 to 2.8 for different weather conditions for houses. In a similar study I. Calixto-Aguirre et. al [28] proposes a validation with RMSE of the order of 2.6 for temperature.

Figure 6 b presents a direct comparison of measured and simulated velocities in an error chart. Reassuringly, the pattern of velocity change across different measurement points within the compartment is identical in both the measured and simulated cases. The measured values for most of the compartment have also been found to be close to the simulated values. However, at some measurement points particularly at T112 and T315, the measured values are significantly higher than the simulated values, but the deviations at these two points are still below 0.12. Although the difference appears large, it is quite justifiable for a simulation model that imitates an actual dynamic scenario with varying environmental and demographic parameters. Moreover the Mean error considering all the measurement points has been found will within 10% range, which can be considered as the validation of the simulation with respect to experimental data.

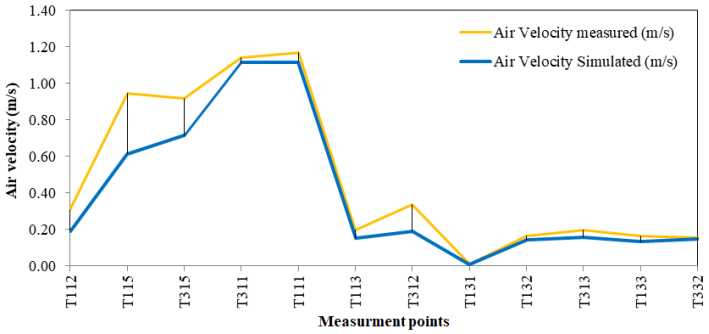

Figure 6. b. The comparision of measured and simulated velocity in an error chart

The measurement points that have shown significant deviation from the measured values, mostly lies near to windows and adjacent area. The simulation considers the inlet air stream to be perpendicular to the window. However, during the real-time operation the local inlet air velocity fluctuations are significantly higher and unpredictable. The velocity of air entering the window is influenced by various environmental and demographic parameters, including the location of the coach within the compartment and the curvature of the railway track, among others.

4. Simulation Results and discussion:

Figure 7 shows the flow of streamlines and the temperature profile within a ventilated coach compartment. The flow profile clearly indicates a highly wind-driven and turbulent airflow inside the coach. Windows act as the primary entrance for the wind, while the overhead vent is the only exit. No significant temperature drop due to inlet air has been recorded anywhere inside the coach; on the contrary, heat plumes can clearly be observed in most parts of the compartment (Figure 8). The regions closer to the coach walls are relatively hotter because of their proximity to those walls. Regarding seating, the upper seats are the hottest, followed by the lower middle seats. The central part of the compartment, which lies just below the overhead vent, is the coolest region. The CFD analysis showed a temperature difference as low as 1.37 degrees between the hottest and coolest regions inside the compartment.

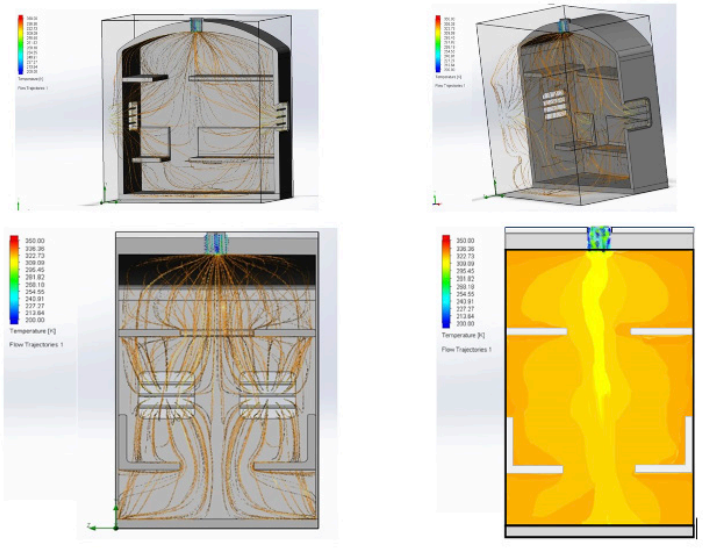

Figure 7. Flow streamlines and temperature profile inside a ventilated coach compartment

The mean air velocity inside the compartment is found to be 0.364 m/s. This value is slightly higher than the ASHRAE standard value which is 0.2 m/s for such ventilated environment [23]. However, the internal geometry of the coach and the turbulent nature of the incoming wind create a significant velocity gradient within the compartment. Probe points T121, T125, T321, and T325 (located

just adjacent to the window) recorded the maximum air velocity inside the compartment. Similarly, the lowest air velocity is observed at probe points T131 and T331. Both points are located on the wall side of the upper luggage rack. Apart from these two locations, the central part of the compartment (toward the aisle) had almost stagnant air. Because air at elevated temperature during summer increases convective heating within an enclosed space, the central region is theoretically the most comfortable zone in the compartment. This has been verified by the field survey conducted by the author where passengers at the aisle seats voted for second most thermal comfort[17].

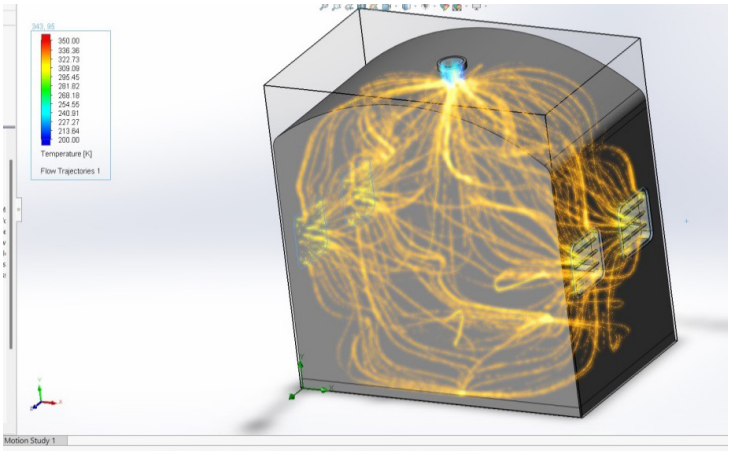

Figure 8. Flow streams depicting heat plumes inside the compartment

However, in the same study, upper seats were reported to have the least thermal comfort, even though the air velocities at these locations are negligible. The CFD results above also highlight these regions as the hottest areas of the compartment, thereby strengthening the previous findings of the field survey. The upper seats (or to be specific, the luggage rack) are mounted at a slightly elevated position to provide comfortable headroom for passengers in the lower seats. This makes the upper seats too close to the ceiling and the side walls. Also, the materials used in making these seats (mainly steel, wood, foam, and resin) are highly prone to conductive and radiative heating.

The air column at the center, when it moves upward towards the exit vent, tends to cool slightly and gain significant speed. Figure 9 shows the variations in velocity and temperature as a function of elevation along the central air column. Up to a height of 1m, a slight fall in temperature is recorded, and velocity remains nearly constant, close to 0.2 m/s, which is the ASHRAE threshold value for thermal comfort. A height of 1 m is also equal to the elevation of the average passenger's face when seated. Hence, theoretically, passengers sitting near this central column should experience higher thermal comfort than others.

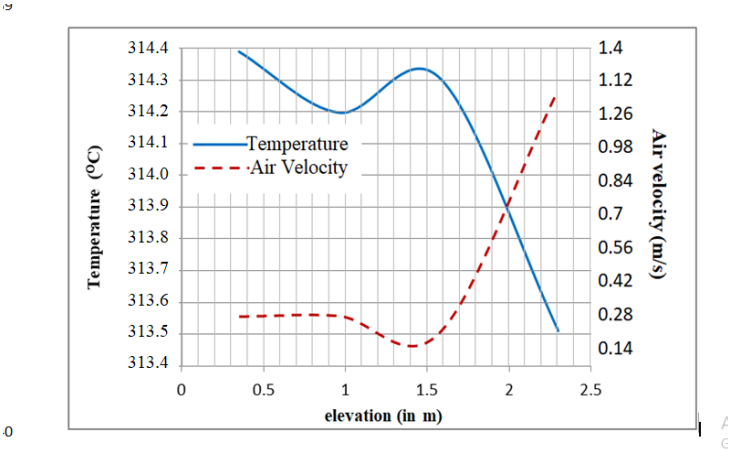

Figure 9. The variation in velocity and temperature with respect to elevation of the central air column

Figure 10 shows trendlines of air velocity fluctuations at different parts of the compartment with respect to elevation, which were again found to validate each other. Since it has already been established that air velocity plays a vital role in manipulating passengers' comfort perception, these trendlines could be beneficial in optimizing the positions of fans and ducts to control proper circulation of cooling air, if any. The trendlines also give an eagle's-eye view of possible PMV (predictive mean vote) of passengers at different locations within the compartment.

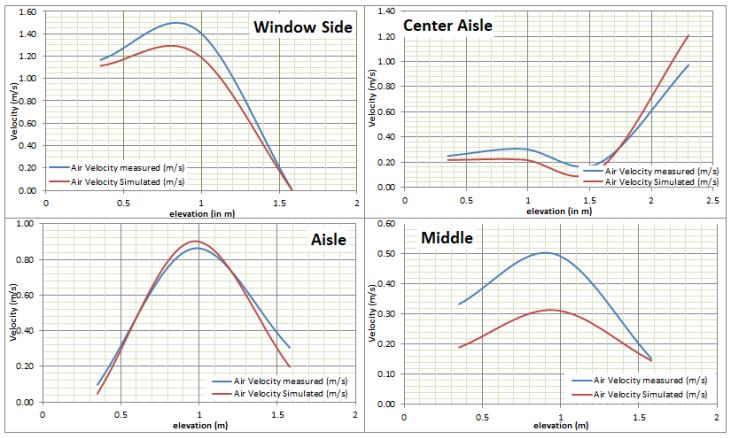

Figure 10. Trendlines of velocity fluctuaction of air at different part of compartment with respect ot elevation

5. Assessment of comfort parameters

Amongst the most common thermal comfort parameter is Fanger's PMV-PPD model[11].This model is basically a predictive model for general, or whole-body, thermal comfort[14]. The base of the model is the heat balance in the human body, i.e., the equilibrium between metabolic heat gain and heat rejection to the environment[15]. In the core of the procedure, it involved the measurements of the pre-

dicted mean vote and the predicted percentage dissatisfied as defined as PMV and PPD respectively [16]. The PMV denotes the expected mean vote of the considered population regarding the thermal environment. The responses were based on a 7-point comfort scale ranging from +3 (too hot) to -3 (too cold), with the comfortable condition at 0(zero) on the scale. The real-time response of passengers regarding their current thermal comfort is termed the thermal sensation vote (TSV). The relationship established by Fanger [18] between PMV and thermal factors is described as:

$$\begin{aligned} PMV = {} & \left(0.352e^{-0.042\left(\frac{M}{F_{Du}}\right)} + 0.032\right)\left\{\frac{M}{F_{Du}}(1 - \eta)\right. \\ & -0.35\left[43 - 0.061\frac{M}{F_{Du}}(1 - \eta) - p_a\right] \\ & -0.42\left[\frac{M}{F_{Du}}(1 - \eta) - 50\right] - 0.0023\frac{M}{F_{Du}}(44 - p_a) \\ & -0.0014\frac{M}{F_{Du}}(34 - t_a) - 3.4 \times 10^{-8} f_{cl}\left[(t_{cl} + 273)^4\right. \\ & \left.\left. - (t_{mrt} + 273)^4\right] - f_{cl} h_c (t_{cl} - t_a)\right\} \end{aligned} \quad (14)$$

Fanger devised an additional equation that relates the PMV to the predicted percentage of dissatisfied (PPD). Once the PMV is evaluated, the PPD, an index that provides a quantitative prediction of the percentage of thermally dissatisfied occupants (i.e., occupants who are too warm or too cold), can be obtained. PPD (figure 11) provides the percentage of individuals predicted to experience local discomfort.

$$PPD = 100 - 95\exp\left(-0.03353 \cdot PMV^4 - 0.2179 \cdot PMV^2\right) \quad (15)$$

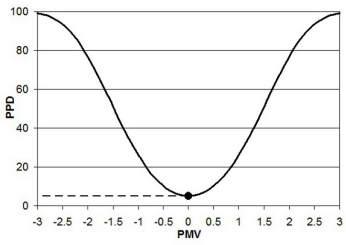

Figure 11. Predicted percentage dissatisfied (PPD)as a function of predicted mean vote (PMV)

Of the previously selected measurement points, 12 key seat locations were identified; the simulated results for these locations were then processed to obtain the (predictive mean vote) PMV values. For these 12 seats, PMV was also calculated based on experimental values, and the results were compared. The mean PMV across all 12 locations was 4.73. Figure 12 below shows a bubble comparison of PMV values for both simulated and experimental results. Simulated PMV has been found to be higher than experimental PMV in most seats. The mean error between experimental and simulated PMV was 7%. The Thermal Sensation Vote at the same measurement points is considerably lower than both PMVs. This has already been explained in the previous paper[17] that the TSV value becomes lower due to thermal adaptation of passengers' and the psychological factors. As stated by Fanger[25], the thermal sensationation of environment is also widely affected by clothing insulation and metabolism rate, both of which are subjective parameters. However, the thermal sensation is not just limited to environmental and subjective parameters, but may also be significantly influenced by psychological factors. For instance, a thermal environment, which is generally considered comfortable, may nevertheless feel uncomfortable to a particular subject. This psychological phenomenon may be influenced by factors, including, but not limited to, gender and age. In light of this, efforts were made to include subjects with a wider range of ages, genders, clothing insulation, and ethnicities in the study.

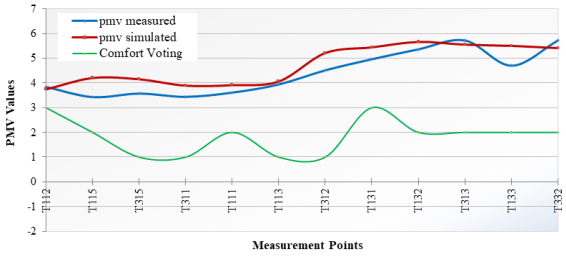

Figure 12. Comparision of PMV values for simulated and experimental results along with TSV

Lower in TSV values in different zones of the compartment are associated with a lower mean predictive percentage of dissatisfaction (PPD) during the field survey. The average PPD in the field survey was 67.33%. On the contrary, the mean PPD based on experimental values is 99.94 % and based on simulated values is 99.99%. This is due to the machine's limitation in interpreting human psychological responses to the thermal comfort of a given ambience. Remarkably, the environmental conditions that are uncomfortable by the standards may feel comfortable to some people, at least to some extent. Figure 13 shows comparision of PPD at different measurement points.

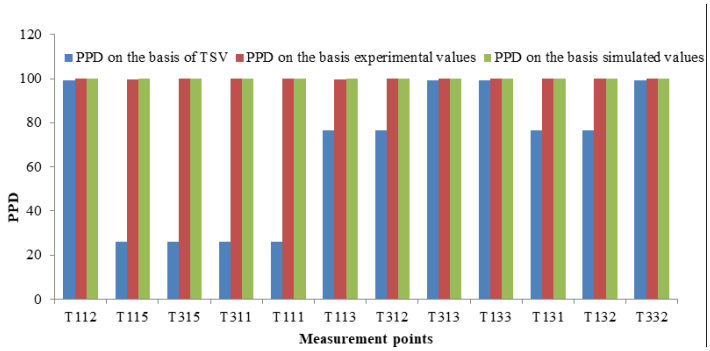

Figure 13. PPD at different measurement points on the basis of TSV, experimental result and software simulation

6. Justification for lower TSV and psychological influence

Thus leaving behind the error for psychological interpretation of simulating machine or the experimental result, following justification for the higher PPD or lower thermal comfort can be precumed:

Passengers' thermal sensation responses are also influenced by local variations in comfort sensation. Since the air stream does not hit all parts of the human body uniformly, some body parts experience higher thermal discomfort than others. This results in localized thermal discomfort in the human body. Generally, passengers sitting toward the window side experience a direct breeze (or draught) on their faces (or upper bodies), while their lower bodies are less influenced by the incoming air stream. This local variation in thermal comfort sensation creates confusion in decision-making, which results in relatively higher thermal comfort sensation votes by passengers.

Since the interior of the coach compartment incorporates different materials with different heat-radiating capabilities, greater radiation asymmetry may be observed. Although the majority of interior walls of the compartment are wood-paneled and thermally insulated, a large number of structural components (such as bars, posts, racks, window frames, etc.) are made of steel, which results in higher thermal radiation inside the coach. On the other hand, a larger surface area of the human body in direct contact with foam cushions causes a radiation gradient and, in turn, influences the passenger's perception of comfort.

Although only a small vertical temperature gradient exists inside the coach, it still significantly influences passengers' psychological perception of thermal comfort. The simulation results are helpful in identifying the zone inside the compartment where this vertical temperature gradient is more significant than in other parts.

For passengers travelling in non airconditioned coach, zone of independence exists for a very narrower range of temperature for most of the air velocity and relative humidity combinations[24]. Draught rate plays a key role in influencing passenger comfort, except in this Zone of Independence.Unfortunately, in a rolling stock with ventillated windows, the draught rate varies abruptly and unperedicably and depends upon the speed of the rolling stock. However considering Fanger's model [25] that corelates the airvelocity and turbulence intensity to predict the draught rate, the zone of optimal thermal comfort inside the coach. As mentioned earlier, the upper seats adjacent to the side walls experience maximum turbulence and are thus mostly affected by the draught rate.

The defined limit for floor temperature is upto 29^{O}C [26], while in our case the measured floor temperature is found to be 30^{O}C. However, floor temperature does not seem to cause significant discomfort to passengers because during travelling most passengers either wear shoes or prefer to raise their feet onto the seats for a comfortable sitting posture.

7.Conclusion

The analysis of airflow and temperature distribution within a ventilated coach compartment reveals several critical insights into passengers' thermal comfort. The flow profile indicates turbulent airflow, primarily driven by wind entering through the windows. The overhead vent in the central part of the coach served as the sole air outlet. Notably, air from the window did not cause any temperature drop inside the coach; instead, heat plumes were prevalent, particularly near the walls. The most affected parts of the coach by the heat plumes are the upper seats, where the temperature is highest. The central area, located beneath the overhead vent, is identified as the coolest zone. The temperature difference between the hotest and the coolest regeion inside the compartment is found to be 1.37^{O}C, which is small but has significant effect on thermal comfort during travelling. Temperature and velocity profiling of railway coaches is crucial and helpful for designing thermally comfortable coaches. The interior of the naturally ventilated railway coach may be redesigned by properly orienting seat placements to improve passengers' thermal comfort. Based on these values, more innovative design approaches may be explored, including variations in coach materials and body-window proportions to improve the thermal comfort of passengers.

Another novel contribution of the research is the simulation of real-time dynamic thermal environment of naturally ventilated railway coaches and the identification of the degree of discomfort experienced by passengers in these coaches. Predictive mean vote (PMV), which is one of the most crucial parameter of thermal comfort is conventionally obtained by conducting a detailed field study and extensive data collection. The study contributes to simulating the PMV with an accuracy as low as 93% in a real-time thermal environment inside a railway coach. This is a major milestone in the prediction of passengers' thermal comfort in a public transport system. In our study, the PMV was 4.73, with a corresponding PPD of 99.99. While the mean standerd effective temperature (SET) for the same has been obtained as 36.65 ^{o}C. All these values translate into a higher degree of discomfort.

The study also found that the mean air velocity within the compartment was 0.364 m/s, which is significantly higher than the ASHRAE standard of 0.2 m/s for ventilated environments. This velocity is influenced by the compartment's internal geometry and the turbulent nature of incoming air. Maximum air velocities occur near the windows, while stagnant air is observed in the central aisle, which, theoretically, should provide greater thermal comfort. However, field surveys indicate that occupants of upper seats, despite lower air velocities, report the least thermal comfort because they are close to the ceiling and because the materials used in their construction are prone to conductive and radiative heating.

The study highlights the importance of localized thermal sensations, as passengers experience varying comfort levels based on their position relative to the airflow and radiant heat sources. Further analysis

of comfort parameters shows that simulated Predicted Mean Vote (PMV) values are generally higher than experimental PMV values, with a mean error of 7%. This discrepancy is attributed to psychological factors influencing perception of thermal comfort and to localized variations in thermal sensation.

Copyright permission statement

All figures included in this manuscript are original works created by the authors. No copyrighted figures, images, or graphical elements from other sources have been used in this manuscript.

List of abbreviations

ICF coach	Integral coach factory coach
CFD	Computational fluid dynamics
ASHRAE	American Society of Heating, Refrigerating and Air Conditioning Engineers
CRIS	Centre of Railway Information System
PMV	Predictive Mean Vote
PPD	Predictive percentage dissatisfaction
VTCE	Virtual Thermal Comfort Engineering
RANS	Reynolds-Averaged Navier-Stokes (RANS)
SUV	Sports Utility Vehicle
S2S	Surface to surface
FANS	Favre-averaged Navier-Stokes
TSV	Thermal Sensation Vote

References

[1] B. Sarkar and R. Mantralaya, "Indian railways annual report and accounts 2019-20," vol. 21, pp. 113–117, 2020.

[2] C. H. Bemisderfer, A. C. Kent, and J. T. Leroy, "ASHRAE Handbook Fundamentals," ASHRAE Inc., 2017, [Online]. Available: https://sovathrothsama.files.wordpress.com/2016/03/ashrae-hvac-2001-fundamentals-handbook.pdf.

[3] Z. Ge, G. Xu, H. J. Poh, C. C. Ooi, and X. Xing, "CFD simulations of thermal comfort for naturally ventilated school buildings," IOP Conf. Ser. Earth Environ. Sci., vol. 238, no. 1, 2019, doi: 10.1088/1755-1315/238/1/012073.

[4] Netam et. al., "Assessing the Impact of Passive Cooling on Thermal Comfort in LIG House using CFD", Journal of Thermal Engineering, Volume: 5, Issue: 414-421, DOI: 10.18186/thermal.623212

[5] PAPER SERIES A Sensitivity Study of Occupant Thermal Comfort in a Cabin Using Virtual Thermal Delphi Thermal and Interior Reprinted From : Climate Control," no. 724, 2018.

[6] C. Suárez, A. Iranzo, J. A. Salva, E. Tapia, G. Barea, and J. Guerra, "Parametric investigation using computational fluid dynamics of the HVAC air distribution in a railway vehicle for representative weather and operating conditions," Energies, vol. 10, no. 8, 2017, doi: 10.3390/en10081074.

[7] A. Eldegwy and E. E. Khalil, "Passengers' thermal comfort in private car cabin in hot climate," 2018 Jt. Propuls. Conf., pp. 1–11, 2018, doi: 10.2514/6.2018-4613.

[8] M. Konstantinov and C. Wagner, "Numerical simulation of the thermal comfort in a model of a passenger car cabin," Notes Numer. Fluid Mech. Multidiscip. Des., vol. 132, no. 3, pp. 383–393, 2016, doi: 10.1007/978-3-319-27279-5_34.

[9] H. Zhang, E. Arens, C. Huizenga, and T. Han, "Thermal sensation and comfort models for non-uniform and transient environments: Part I: Local sensation of individual body parts," Build. Environ., vol. 45, no. 2, pp. 380–388, 2010, doi: 10.1016/j.buildenv.2009.06.018.

[10] M. Siodlaczek, M. Gaedtke, S. Simonis, M. Schweiker, N. Homma, and M. J. Krause, "Numerical evaluation of thermal comfort using a large eddy lattice Boltzmann method," Build. Environ., vol. 192, no. December 2020, p. 107618, 2021, doi: 10.1016/j.buildenv.2021.107618.

[11] M. Konstantinov and C. Wagner, "Flow and thermal comfort simulations for double decker train cabins with passengers," Civil-Comp Proc., vol. 110, no. December, 2016, doi: 10.4203/ccp.110.42.

[12] Y. Tang, H. Yu, Z. Wang, M. Luo, and C. Li, "Validation of the stolwijk and tanabe human thermoregulation models for predicting local skin temperatures of older people under thermal transient conditions," Energies, vol. 13, no. 24, 2020, doi: 10.3390/en13246524.

[13] P. Danca, I. Nastase, F. Bode, C. Croitoru, A. Dogeanu, and A. Meslem, "Evaluation of the thermal comfort for its occupants inside a vehicle during summer," IOP Conf. Ser. Mater. Sci. Eng., vol. 595, no. 1, 2019, doi: 10.1088/1757-899X/595/1/012027.

[14] W. Liu, Q. Deng, W. Huang, and R. Liu, "Variation in cooling load of a moving air-conditioned train compartment under the effects of ambient conditions and body thermal storage," Appl. Therm. Eng., vol. 31, no. 6–7, pp. 1150–1162, 2011, doi: 10.1016/j.applthermaleng.2010.12.010.

[15] A. R. Tupe, "Maintenance Manual for Builders," Minist. Railw. Bharat Sarkar, vol. 474005, 2015, [Online]. Available: https://rskr.irimee.in/training-material.

[16] S. Srikrishna, "Construction of coach body," 2022. [Online]. Available: https://rskr.irimee.in/sites/default/files/ICF Coach Shell.pdf.

[17] S. S. Mishra, V. K. Gaba, and N. Netam, "Thermal comfort assessment of non air-conditioned railway coach in Central India during extreme summer," Therm. Sci. Eng. Prog., vol. 46, no. January, p. 102206, 2023, doi: 10.1016/j.tsep.2023.102206.

[18] J. Srebric, V. Vukovic, G. He, and X. Yang, "CFD boundary conditions for contaminant dispersion , heat transfer and airflow simulations around human occupants in indoor environments," vol. 43, pp. 294–303, 2008, doi: 10.1016/j.buildenv.2006.03.023.

[19] C. K. G. Lam and K. Bremhorst, "A modified form of the k-ε model for predicting wall turbulence," J. Fluids Eng. Trans. ASME, vol. 103, no. 3, pp. 456–460, 1981, doi: 10.1115/1.3240815.

[20] M. Konstantinov and C. Wagner, "Numerical simulation of the air flow and thermal comfort in a train cabin," Civil-Comp Proc., vol. 104, no. July 2016, 2014, doi: 10.4203/ccp.104.328.

[21] X. Kong, Y. Chang, N. Li, H. Li, and W. Li, "Comparison study of thermal comfort and energy saving under eight different ventilation modes for space heating," Build. Simul., vol. 15, no. 7, pp. 1323–1337, 2022, doi: 10.1007/s12273-021-0814-7.

[22] I. B. Celik, U. Ghia, P. J. Roache, C. J. Freitas, H. Coleman, and P. E. Raad, "Procedure for estimation and reporting of uncertainty due to discretization in CFD applications," J. Fluids Eng. Trans. ASME, vol. 130, no. 7, pp. 0780011–0780014, 2008, doi: 10.1115/1.2960953.

[23] E. Arens, S. Turner, H. Zhang, and G. Paliaga, "Moving air for comfort," ASHRAE J., vol. 51, pp. 18–28, May 2009.

[24] S. S. Mishra, V. K. Gaba, and N. Netam, "Effect of air velocity and relative humidity on passengers' thermal comfort in naturally ventilated railway coach in hot-dry indian climate," Build. Environ., vol. 254, no. March, p. 111421, 2024, doi: 10.1016/j.buildenv.2024.111421.

[25] P. O. Fanger, A. K. Melikov, H. Hanzawa, and J. Ring, "Air turbulence and sensation of draught," Energy Build., vol. 12, no. 1, pp. 21–39, 1988, doi: 10.1016/0378-7788(88)90053-9.

[26] ASHRAE, "ANSI/ASHRAE Addenda o, p, and to ANSI/ ASHRAE Standard 55-2010," vol. 8400, p. 7, 2013, [Online]. Available: www.ashrae.org.

[27] Netam, N., Sanyal, S., & Bhowmick, S.(2020)."A mathematical model featuring time lag and decrement factor to assess indoor thermal conditions in low-income-group house", Journal of Thermal Engineering, 6(2),114-127. https://doi.org/10.18186/thermal.728054.

[28] I. Calixto-Aguirre et. al., "Validation of thermal simulations of a non-air-conditioned office building in different seasonal, occupancy and ventilation conditions", Journal of Building Engineering,Volume 44, 2021, doi:10.1016/j.jobe.2021.102922

[29] Ye, X J , et. al. "Field study of thermal environment in trains", Indoor Air 2005: Proceedings of the 10th International Conference on Indoor Air Quality and Climate, Vols 1-5

[30] Wang C et. al., "Thermal environment and thermal comfort in metro systems: A case study in severe cold region of China", Building and Environment, 227, doi: 2023 10.1016/j.buildenv.2022.109758

[31] Zhang, Y. et. al, "Experimental investigation into the effects of different metabolic rates of body movement on thermal comfort" Building and Environment, vol. 10,page 168, 2019, doi: 10.1016/j.buildenv.2019.106489

[32] Alam, M. S., & Salve, U. R.. Factors affecting on human thermal comfort inside the kitchen area of railway pantry car-a review. Journal of Thermal Engineering, 7(Supp 14),2093-2106, 2021